View metadata, citation and similar papers at core.ac.uk

brought to you by CORE

provided by Institutional Repository of Institute of Earth Environment, CAS

Organic Geochemistry 115 (2018) 24–31

Contents lists available at ScienceDirect

Organic Geochemistry

journal homepage: www.elsevier.com/locate/orggeochem

# Microbial production of long-chain *n*-alkanes: Implication for interpreting sedimentary leaf wax signals

Gaoyuan Li [a,b,*], Li Li [c], Rafael Tarozo [b], William M. Longo [b], Karen J. Wang [b], Hailiang Dong [a,d], Yongsong Huang [b,e,*]

[a] State Key Laboratory of Biogeology and Environmental Geology, China University of Geosciences, Beijing 100083, China
[b] Department of Earth, Environmental and Planetary Sciences, Brown University, Providence, RI 02912, USA
[c] State Key Laboratory of Marine Geology, Tongji University, Shanghai 200092, China
[d] Department of Geology and Environmental Earth Science, Miami University, Oxford, OH 45056, USA
[e] Institute of Earth Environment, Chinese Academy of Sciences, Xi'an 710075, China

ARTICLE INFO

*Article history:*
Received 15 August 2017
Received in revised form 30 September 2017
Accepted 10 October 2017
Available online 21 October 2017

*Keywords:*
Long-chain *n*-alkanes
Leaf-wax
Microbial production
Deuterium-enrichment incubation
Compound specific hydrogen isotope ratios

ABSTRACT

Relative distributions as well as compound-specific carbon and hydrogen isotope ratios of long-chain $C_{25}$ to $C_{33}$ *n*-alkanes in sediments provide important paleoclimate and paleoenvironmental information. These compounds in aquatic sediments are generally attributed to leaf waxes produced by higher plants. However, whether microbes, such as fungi and bacteria, can make a significant contribution to sedimentary long-chain *n*-alkanes is uncertain, with only scattered reports in the early 1960s to 1970s that microbes can produce long-chain *n*-alkanes. Given the rapidly expanding importance of leaf waxes in paleoclimate and paleoenvironmental studies, the impact of microbial contribution to long-chain *n*-alkanes in sediments must be fully addressed. In this study, we performed laboratory incubation of peatland soils under both anaerobic and aerobic conditions in the absence of light with deuterium-enriched water over 1.5 years and analyzed compound-specific hydrogen isotopic ratios of *n*-alkanes. Under aerobic conditions, we find *n*-alkanes of different chain length display variable degrees of hydrogen isotopic enrichments, with short-chain ($C_{18}$–$C_{21}$) *n*-alkanes showing the greatest enrichment, followed by long-chain "leaf wax" ($C_{27}$–$C_{31}$) *n*-alkanes, and minimal or no enrichment for mid-chain ($C_{22}$–$C_{25}$) *n*-alkanes. In contrast, only the shorter chain ($C_{18}$ and $C_{19}$) *n*-alkanes display appreciable isotopic enrichment under anaerobic conditions. The degrees of isotopic enrichment for individual *n*-alkanes allow for a quantitative assessment of microbial contributions to *n*-alkanes. Overall our results show the microbial contribution to long-chain *n*-alkanes can reach up to 0.1% per year in aerobic conditions. For shorter chain *n*-alkanes, up to 2.5% per year could be produced by microbes in aerobic and anaerobic conditions respectively. Our results indicate that prolonged exposure to aerobic conditions can lead to substantial accumulation of microbially derived long-chain *n*-alkanes in sediments while original *n*-alkanes of leaf wax origin are degraded; hence caution must be exercised when interpreting sedimentary records of long-chain *n*-alkanes, including chain length distributions and isotopic ratios.

© 2017 Elsevier Ltd. All rights reserved.

## 1. Introduction

Long-chain ($C_{25}$–$C_{33}$) *n*-alkanes are important biomarkers for terrestrial plants in aquatic sediments, providing important information for paleo-environment and paleo-climate reconstructions (Eglinton and Hamilton, 1967; Huang et al., 2001; Castañeda and Schouten, 2011; Schefuß et al., 2011; Sachse et al., 2012; Bush and McInerney, 2013; Konecky et al., 2014; Rach et al., 2014; Wang et al., 2016). For example, compound-specific carbon isotopic compositions have been used to understand past vegetation assemblages ($C_3$ vs $C_4$ plants) (Huang et al., 1999, 2007; Eglinton and Eglinton, 2008; Tipple et al., 2011; Russell et al., 2014). Hydrogen-isotopic ratios of individual waxes have been used to understand hydrological changes over different geological time scales (Huang et al., 2004; Pagani et al., 2006; Hou et al., 2008;

* Corresponding authors at: State Key Laboratory of Biogeology and Environmental Geology, China University of Geosciences, Beijing 100083, China (G. Li), Department of Earth, Environmental and Planetary Sciences, Brown University, Providence, RI 02912, USA (Y. Huang).

*E-mail addresses:* ligy@cugb.edu.cn (G. Li), yongsong_huang@brown.edu (Y. Huang).

https://doi.org/10.1016/j.orggeochem.2017.10.005
0146-6380/© 2017 Elsevier Ltd. All rights reserved.

Tierney et al., 2008; Polissar et al., 2009; Konecky et al., 2011; Sachse et al., 2012; Thomas et al., 2016).

Accurate paleoclimate and paleoenvironmental interpretation of leaf wax *n*-alkanes relies on the assumption that these biomarkers are exclusively derived from higher plants (Lichtfouse et al., 1995; Huang et al., 2002; Pancost et al., 2002; Meyers, 2003; Schefuß et al., 2005; Huang et al., 2007; Tipple and Pagani, 2010; Tipple et al., 2011). However, there have been scattered reports in the 1960–1970s that microbes, e.g., fungi and bacteria can also produce long-chain *n*-alkanes. For instance, Orò et al. (1966) reported the chlamydospores of *Ustilago maydis*, *U. nuda*, and *Sphacelotheca reiliana*, collected from surrounding exterior surfaces of higher plant tissues, contain *n*-alkanes ranging from $C_{14}$ to $C_{37}$, with principal hydrocarbons *n*-$C_{27}$, *n*-$C_{29}$ and *n*-$C_{31}$ showing an odd numbers of carbon atoms predominance (Orò et al., 1966). However, there are significant uncertainties whether the reported long-chain *n*-alkanes are actually produced by these fungi or acquired from plants or perhaps even accidentally during sampling process (Weete, 1972). In addition, Jones (1969) reported pure cultures of some fungal species including *Penicillium* sp., *Aspergillus* sp., and *Trichoderma viride*, grown in a basal succinate medium and tryptone soya broth respectively, contain *n*-alkanes chain length from $C_{15}$ to $C_{36}$ with major components ranging from *n*-$C_{27}$ to *n*-$C_{30}$ (Jones, 1969). Interestingly, CPI values are between 0.54–1.12, much smaller than observed in higher plants (CPI > 5) (Bush and McInerney, 2013). Jones (1969) also reported some aerobic bacteria, such as *Micrococcus* sp., *Corynebacterium* sp., *Bacillus* sp., and *Mycobacterium* sp., can produce $C_{14}$–$C_{36}$ *n*-alkanes with major components ranging from *n*-$C_{27}$ to *n*-$C_{29}$, and similarly with low CPI values in the range 0.60–1.34. However, the paper did not examine if the growth medium contained any *n*-alkanes.

Although direct analysis of individual microbes is useful for understanding their *n*-alkane production, the results may bear significant uncertainties since leaf waxes are ubiquitous in nature and microbes can attain long-chain *n*-alkanes via contact or ingestion. Additionally, because most of the microbes in the natural environment can't be, or have not been, cultured successfully, it is difficult to determine microbial contributions of long-chain *n*-alkanes in the natural environment through pure culture experiments. The best approach to assess microbial production of long-chain *n*-alkanes is thus to detect their productions in soils in situ (Tu et al., 2011; Zech et al., 2011, 2013). For example, a recent study by Zech et al. (2011), based on changes in δD values of long-chain *n*-alkanes in a 27-month leaf litter degradation experiment, suggested that the contribution of microbially synthesized long-chain *n*-alkanes increased over time and they proposed can reach as much as 30%. However, the assessment was made using relatively small source water δD differences (10–20‰ VSMOW), hence the error for quantifying microbial production of long-chain *n*-alkanes can be substantial, given the relatively high analytical error for individual *n*-alkane δD values and potential sample inhomogeneity (Zech et al., 2011).

To clarify the uncertainties from previous studies, we designed an isotope labeling experiment to: (1) incubate soils in the absence of light (to prohibit photosynthesis), so that all *n*-alkanes produced are from microbial sources with no ambiguity; (2) add 1.5% of heavy water to the incubation (the resulting water has a δD value of 95,195‰ VSMOW), so that even minute amount of microbial production is detectable; (3) based on isotope enrichment over a known period of time, accurately quantify the microbial contribution rate of long-chain *n*-alkanes in natural soils where input and degradation of long-chain *n*-alkanes exist simultaneously.

## 2. Material and methods

### 2.1. Soil sampling and microbial incubation

#### 2.1.1. Sampling site and soil collection

We collected peaty soil samples from surface layer of a wetland located in Glocester (Rhode Island, USA; 41°52′12″N, 71°41′08″W) on June 21, 2014. Peaty soil was selected for this study due to its high organic content, which allowed us to maximize the production of heterotrophic microbes during subsequent laboratory incubation. Approximately 1 L surface 10 cm peaty soil was taken using a 2 L glass bottle with 10 cm diameter. In this area, average elevation is around 139 m above sea level, and the dominant vegetation is *Sphagnum* spp., and accompanied by *Chamaedaphne calyculata*, *Vaccinium macrocarpon*, *Vaccinium corymbosum* and *Acer rubrum*. The mean annual precipitation is around 2600 mm (online meteorological data), with δD value about −51‰ (from online isotope precipitation calculator: http://wateriso.utah.edu/waterisotopes/pages/data_access/form.html).

#### 2.1.2. Microbial incubation

Soil samples were brought to Brown University. On the same day, in a glove box with nitrogen gas, about 80 mL of peaty soil was transferred into a 200 mL beaker, followed by mixing and homogenizing with an additional 50 mL of $O_2$-free distilled deionized water (boiled for 30 min and purged with the $N_2$ bubble for 30 min). After homogenizing, approximately 20 mL of the soil and slurry was transferred into a 40 mL glass vial, tightly capped under an atmosphere of nitrogen (nitrogen gas was blown into the overhead space prior to capping), serving as the control sample of the overall incubation experiment. Subsequently, 1.2 mL $O_2$-free ($N_2$ bubbled for 30 min) 99.8% $D_2O$ (Sigma-Aldrich, ISOTEC Inc., Miamisburg, OH, USA) was added into the remaining slurry of the 200 mL beaker and mixed thoroughly, and a 1 mL slurry water was taken for stable hydrogen isotope ratio analysis. Two experimental subsamples were transferred into two 40 mL vials, each with 20 mL slurry (i.e., the slurry with deuterium water). One 40 mL vial was capped tightly in the glove box and stood upside down outside the glove box to maintain anaerobic condition during the whole process of microbial incubation: there was approximately 1 cm of water over the top of the soil (Supplementary Fig. S1). The other 40 mL vial, designated as aerobic incubation, was opened and shaken up and down multiple times daily to make sure the space air was fully re-saturated with ambient level of oxygen. Afterwards, the aerobic vial was recapped to avoid water evaporation, which can result in changes in water hydrogen isotope ratios. During the whole course of laboratory incubation, all 3 vials were fully covered by aluminium foil (i.e., to keep the incubation with no light hence no photosynthesis) and under room temperature (~20 °C). We conducted our experiments in the dark to avoid any potential growth of photosynthetic vascular plants that are known to make long-chain leaf wax *n*-alkanes. Therefore, our experimental results should be interpreted to only include heterotrophic and chemoautotrophic microorganisms (i.e., photosynthetic organisms were excluded). The whole incubation experiment lasted 540 days.

### 2.2. Hydrogen isotope analysis for deuterium-enriched water

The water δD measurement was carried out using the same procedure as described in Gao et al. (2012). Specifically, the measurement was conducted in a model L1102-I isotopic liquid water and water vapor analyzer (Picarro, Sunnyvale, CA, USA). To ensure the removal of organic matter, 4 mg of activated charcoal was added into the tube with deuterium-enriched slurry water, the water hand-shaken for 1 min and centrifuged at 5000 rpm for 1 min;

the supernatant liquor was filtered (0.22 μm PTEE filters) prior to isotopic measurement. The deuterium-enriched water was diluted with deionized water with known δD value (−43‰ VSMOW) by about 1000 times, so that measured value was close to the range of the isotopic standards. The δD value of original deuterium-enriched water was determined as 95,195‰ VSMOW (i.e., 1.5% $D_2O$), base on a hydrogen isotope mass balance function (Gao et al., 2012).

### 2.3. Lipids extraction, purification and analysis

At the end of incubation experiment, three samples (control, aerobic and anaerobic incubation) were freeze-dried. The freeze-dried peat samples (5–6 g of total sample in the vials) were extracted using an accelerated solvent extractor (ASE200, Dionex) with dichloromethane/methanol mixture (9:1, v:v) at 120 °C and 1200 psi. The total lipids were then separated into neutral and acid fractions using solid-phase extraction column packed with aminopropylsilyl (i.e., silica gel with amine groups) with dichloromethane:isopropanol (2:1, v:v) and 4% AcOH in $Et_2O$ as the respective eluents. To isolate the hydrocarbons, the neutral fractions were further separated over pre-cleaned silica gel columns and eluted with hexane (Gao et al., 2012).

Concentrations of individual compounds of hydrocarbons were determined using gas chromatography (6890 gas chromatograph; Agilent Technologies, Santa Clara, CA, USA) with split/split-less injection and flame ionization detection (FID). A 30 m capillary column (HP-1MS, 0.32 mm i.d., 0.25 μm film thickness; Agilent) and an auto-sampler (HP7683) were used. The carrier gas (hydrogen) flow was 1.7 mL/min. The temperature was set as follows: 60 °C (1 min) to 220 °C at 20 °C/min then to 315 °C (held 15 min) at 6 °C/min. Compounds of each fraction were quantified based on internal standard (hexamethylbenzene) added into each sample vial prior to GC-FID analyses, and the compounds were identified by comparison with retention times and mass spectra from GC–MS analyses (Agilent 5973N quadrupole mass spectrometer interfaced to an Agilent 6890N GC) based on previous methods (Gao et al., 2011, 2012). Average chain length (ACL) and carbon preference index (CPI) were calculated using the following equations:

$$ACL = \Sigma(C_n \times n)/\Sigma(C_n) \quad (1)$$

$$CPI = [\Sigma_{odd}(C_{21-29}) + \Sigma_{odd}(C_{23-31})]/(2\Sigma_{even}C_{22-30}) \quad (2)$$

where $C_n$ is the concentration of each *n*-alkane with *n* carbon atoms.

The hydrogen isotope ratios of *n*-alkanes were measured using HP 6890 GC (Agilent Technologies) interfaced to a Finnigan MAT Delta+ XL isotope ratio mass spectrometry (IRMR) through a high temperature pyrolysis reactor. The $H_3^+$ factor was determined every other day prior to sample runs. The precision of standard triplicate analyses was within ± 3‰. To ensure no isotopic drift, external standards with known δD values (mixture of $C_{25}$, $C_{27}$, $C_{29}$ and $C_{31}$ *n*-alkanes) were injected 3× prior to sample analysis after every three sample injections. Because the δD values of individual compounds in our samples presumably encompass a wide range, a possible isotopic memory effect should be considered during hydrogen isotope ratio measurement (Wang and Sessions, 2008). Wang and Sessions (2008) reported that when two compounds elute closely on GC–IRMS (e.g., when they differ by one carbon number in an *n*-alkane series) hydrogen isotopic value of a preceding compound can affect a later eluting compound by 2–4% of the isotopic difference. In our case of $C_{18}$ and $C_{19}$ *n*-alkanes, the isotopic difference is ~1400‰. Hence the maximal memory effect on $C_{19}$ *n*-alkane would be 56‰. These highly enriched δD values do not affect the isotopic values of long-chain *n*-alkanes since our $C_{22}$ and $C_{23}$ *n*-alkanes display very low δD values (Table 2, Fig. 2). Therefore, the potential minor isotopic memory effect during GC–IRMS analysis reported by Wang and Sessions (2008) does not significantly affect the interpretation of our results.

## 3. Results

### 3.1. Abundances of n-alkanes in peat samples

Distributions and abundances of *n*-alkanes are shown in Fig. 1 and Table 1. *n*-Alkanes display a typical odd over even predominance (Fig. 1), with maximal carbon numbers at *n*-$C_{29}$. The concentrations of short-chain ($C_{18}$–$C_{21}$) *n*-alkanes are 0.05–0.1 μg/g dry weight (μg/gdw), followed by medium- and long-chain *n*-alkanes ($C_{22}$–$C_{28}$; 0.1–0.6 μg/gdw). The concentrations of the dominant long-chain *n*-alkanes ($C_{29}$ and $C_{31}$) are 0.8–1.8 μg/gdw.

The differences of homolog distributions, including concentrations, carbon preference index (CPI) and average chain length (ACL) among the three samples are not evident, with ACL 27.0 and CPI 5.9 for the control sample, ACL 27.3 and CPI 6.5 for the anaerobic incubated sample, and ACL 26.9 and CPI 5.5 for the aerobic incubated sample (Table 1).

### 3.2. D/H ratios of n-alkanes

The average δD values and standard deviations from three duplicated measurements of individual compounds for the three samples are shown in Table 2. The δD values of *n*-alkanes for the control sample (i.e., the sample not incubated in D-enriched water) are −201‰ to −140‰ for short-chain length ($C_{18}$–$C_{21}$) *n*-alkanes, and −224‰ to −125‰ for medium-chain ($C_{22}$–$C_{25}$), −121‰ to −96‰ for long-chain ($C_{26}$–$C_{31}$), except for $C_{27}$ *n*-alkane whose the unusually high δD value of *n*-$C_{27}$ (−57‰) is likely caused by an unknown co-eluting compound. Compared with the control sample, under aerobic conditions, *n*-alkanes of different chain length display variable degrees of hydrogen isotopic enrichments, with short-chain ($C_{18}$, $C_{19}$, $C_{20}$ and $C_{21}$) *n*-alkanes showing the greatest enrichment, i.e. 3732‰, 2344‰, 466‰ and 363‰ enrichment, respectively, followed by long-chain "leaf wax" ($C_{26}$, $C_{27}$, $C_{29}$ and $C_{31}$) *n*-alkanes with 9‰, 49‰, 97‰, 140‰ and 11‰ enrichment respectively, and minimal or no enrichment for mid-chain

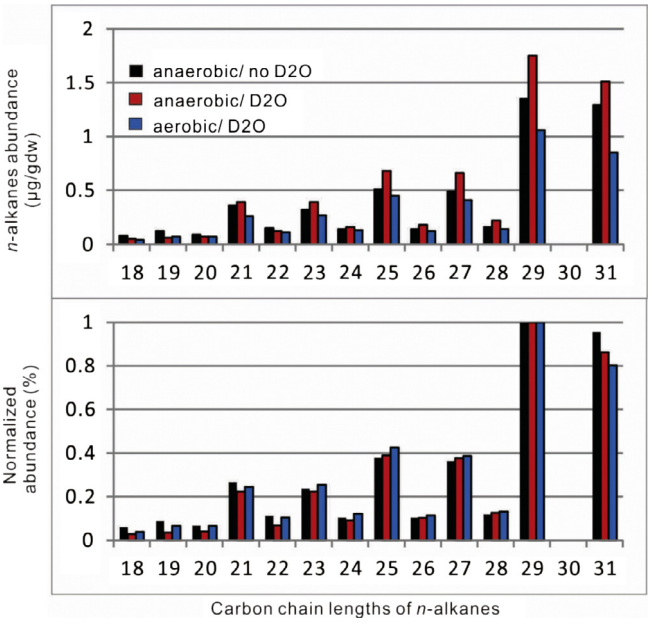


**Fig. 1.** Concentration and chain length distribution of *n*-alkanes in three incubated peaty soil samples.

**Table 1**
Abundance of *n*-alkanes.

| Carbon number | Control | Anaerobic incubation | Aerobic incubation |
|---|---|---|---|
| *n-alkanes (μg/gdw)* | | | |
| 18 | 0.08 | 0.05 | 0.04 |
| 19 | 0.12 | 0.06 | 0.07 |
| 20 | 0.09 | 0.07 | 0.07 |
| 21 | 0.36 | 0.39 | 0.26 |
| 22 | 0.15 | 0.12 | 0.11 |
| 23 | 0.32 | 0.39 | 0.27 |
| 24 | 0.14 | 0.16 | 0.13 |
| 25 | 0.51 | 0.68 | 0.45 |
| 26 | 0.14 | 0.18 | 0.12 |
| 27 | 0.49 | 0.66 | 0.41 |
| 28 | 0.16 | 0.22 | 0.14 |
| 29 | 1.35 | 1.75 | 1.06 |
| 30 | 0.00 | 0.00 | 0.00 |
| 31 | 1.29 | 1.51 | 0.85 |
| *ACL and CPI* | | | |
| ACL | 27.0 | 27.3 | 26.9 |
| CPI | 5.9 | 6.5 | 5.5 |

($C_{22}$, $C_{23}$, $C_{24}$ and $C_{25}$) (Table 2, Fig. 2). In contrast, under anaerobic condition, only the chain lengths $C_{18}$, $C_{19}$, $C_{25}$ and $C_{27}$ *n*-alkanes display appreciable isotopic enrichment, with 906‰, 102‰, 14‰ and 25‰ increases, respectively (Table 2, Fig. 2).

## 4. Discussion

### 4.1. n-Alkane abundance, deuterium enrichment and estimation for chemical hydrogen exchange rate

The abundance and distributions of *n*-alkanes in control, anaerobic and aerobic samples show negligible differences (Fig. 1). The small differences between the samples are most likely due to intrinsic sample inhomogeneity and/or measurement errors. Even for compounds that have maximal microbial productions (like short-chain *n*-alkanes as discussed below), we did not observe systematic differences in concentrations and distributions. Therefore, it is unreliable to use abundances and relative distributions to estimate the microbial production of *n*-alkanes.

One important question for the D-enrichment of *n*-alkanes is whether or not the observed isotopic change is solely due to chemical isotopic exchange between organic hydrogen and deuterium-ion in the water over the course of 1.5 years. Based on the design and results of our incubation experiment, we conclude that direct chemical hydrogen exchange between *n*-alkanes and water is negligible due to the following two reasons: (1) If hydrogen exchange is evident in *n*-alkanes, it should have a similar effect on all *n*-alkanes with different carbon lengths, and as well as for anaerobic and aerobic incubations. However, unlike their shorter and longer chain *n*-alkane homologues, $C_{22}$, $C_{23}$, $C_{24}$ and $C_{25}$ *n*-alkanes do not display evidence of D-enrichment. There are also major differences in the pattern of D-enrichment for *n*-alkanes in aerobic and anaerobic incubations; (2) As described below, chemical hydrogen exchange rate between hydrogens of *n*-alkanes and surrounding water, estimated using published data (Sessions et al., 2003), are extremely low.

Since alkyl H atoms in *n*-alkanes are covalently linked to carbon atoms, a high activation energy is required for exchange (Schimmelmann et al., 1999; Fuller and Huang, 2003; Sessions et al., 2003; Reeves et al., 2012). Sessions et al. (2003) estimated the exchange rates of icosane at different temperature, through incubation on clean montmorillonite or microcrystalline silica. They concluded that the reaction half-times ($t_{1/2}$) for hydrogen exchange in icosane is about $1 \times 10^4$–$1 \times 10^5$ years at 20 °C. For the H/D exchange reaction of *n*-alkanes, $RH_\alpha + D_2O \rightarrow RD_\alpha + HDO$, can be characterized by a pseudo first-order rate law equation (Wedeking and Hayes, 1983; Fuller and Huang, 2003).

$$Kt = \ln[(F_i - F_e)/(F_t - F_e)] \quad (3)$$

$$K = \ln 2/t_{1/2} \quad (4)$$

where $K$ is the rate constant for hydrogen, $t$ is time (which equals to 1.5 years at the end of our incubation experiment). $F_i$ is the initial fractional abundance of deuterium [D/(D + H)] in the corresponding compound, which can be obtained from δD values of compounds in the control sample. $F_t$ is the final fractional abundance of deuterium at time $t$. $F_e$ is the fractional abundance of deuterium of *n*-alkanes when it reaches equilibrium, which can be assumed to be the concentration of the heavy water in our incubation system (i.e., 1.5%). $t_{1/2}$ is between $1 \times 10^4$–$1 \times 10^5$ years (Sessions et al., 2003). Using the Eqs. (3) and (4), we obtain the maximum possible increase in δD value due to chemical hydrogen exchange at room temperature is between 1–10‰ over the whole incubation period (i.e., 1.5 years). This value is much smaller than those observed in our heavy water incubated samples (Table 2, Fig. 2). We therefore conclude that

**Table 2**
Hydrogen isotopic composition of individual compounds.

| Carbon chain length of *n*-alkanes | No $D_2O$ | | 1.5% $D_2O$ | | | |
|---|---|---|---|---|---|---|
| | Control | | Anaerobic incubation | | Aerobic incubation | |
| | δD[a] (‰) | σ[b] (‰) | δD (‰) | σ (‰) | δD (‰) | σ (‰) |
| 18 | −140 | N.D.[c] | 766 | 1.3 | 3592 | 82.0 |
| 19 | −178 | N.D. | −76 | 47.5 | 2166 | 67.4 |
| 20 | −140 | N.D. | N.D. | N.D. | 326 | 3.2 |
| 21 | −201 | 2.2 | −320 | 16.8 | 162 | 75.7 |
| 22 | −125 | 5.4 | −207 | 48.1 | −219 | 12.5 |
| 23 | −182 | 2.3 | −226 | 5.3 | −171 | 3.2 |
| 24 | −224 | 46.5 | −202 | 13.2 | −194 | 3.7 |
| 25 | −177 | 0.9 | −163 | 6.7 | −168 | 1.8 |
| 26 | −96 | 17.8 | −100 | 10.9 | −47 | 6.8 |
| 27 | −57 | 3.3 | −32 | 15.8 | 40 | 2.9 |
| 28 | N.D. | N.D. | N.D. | N.D. | N.D. | N.D. |
| 29 | −107 | 0.9 | −111 | 1.5 | 33 | 2.3 |
| 30 | N.D. | N.D. | N.D. | N.D. | N.D. | N.D. |
| 31 | −121 | 21.2 | −132 | 4.0 | −110 | 2.8 |

[a] δD values are expressed in ‰ relative to VSMOW.
[b] σ = standard derivation of three replicate measurements.
[c] N.D. = not determined.

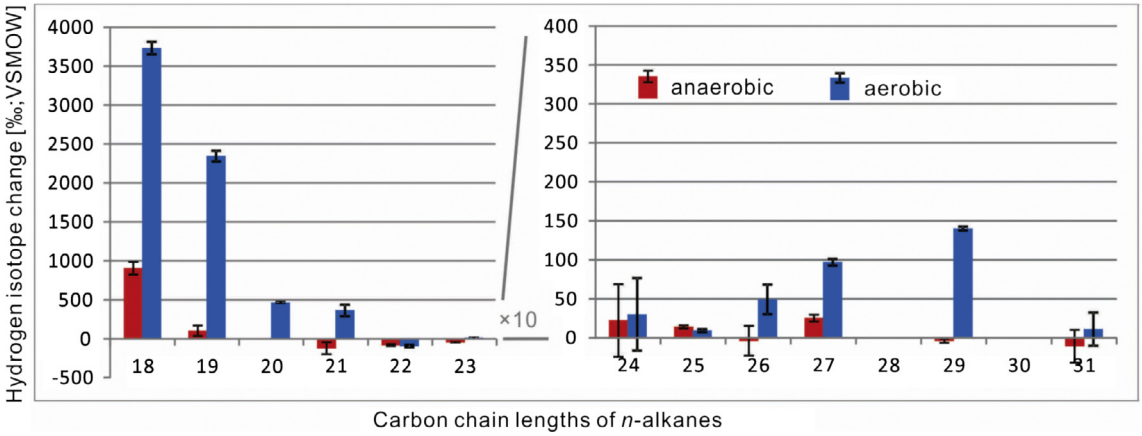


**Fig. 2.** Hydrogen isotopic enrichment degrees of individual *n*-alkanes in two aerobic and anaerobic deuterium-incubated peaty soil samples.

direct chemical D/H exchange between *n*-alkanes and water can be neglected in our incubation experiment.

### 4.2. Microbial production rates of individual n-alkanes

The microbial production rates of individual *n*-alkanes are calculated based on a binary isotope mass balance model as described in Gao et al. (2012). The hydrogen isotope fractionation factors between individual *n*-alkanes and environmental water ($\varepsilon_{n\text{-alkane-water}}$) were evaluated using the $\delta D_{n\text{-alkane}}$ values of compounds in the control sample and $\delta D_{precipitation}$ (i.e. −51‰; average precipitation δD value):

$$\varepsilon_{n\text{-alkane-water}} = (\delta D_{n\text{-alkane}} + 1)/(\delta D_{precipitation} + 1) - 1 \quad (5)$$

The biological fractionation factors between individual lipids and environmental water for microbes in soil are complex (Zhang et al., 2009; Osburn et al., 2011; Sachse et al., 2012) and can be highly variable (Sessions et al., 2002). For simplicity, we assume the fractionation factor is a constant and equals the fractionation of the $C_{18}$ *n*-alkane, because *n*-$C_{18}$ is the most dramatically D labeled compound in our experiment, and generally not produced by higher plants. The $\varepsilon_{n\text{-alkane-water}}$ value is determined as −94‰, by using the measured δD value of $C_{18}$ *n*-alkane in the control sample (−140‰) and the average precipitation δD value of our sampling site (−51‰). Note that the small variation in the absolute values of microbial fractionation factor has little influence on the outcome of production rates (Gao et al., 2012), because of the very high δD value of labeled water.

Based on the fractionation factor ($\varepsilon_{n\text{-alkane-water}}$), the δD value of newly produced *n*-alkanes ($\delta D_{new}$) can be calculated from the δD value of the deuterium-enriched water ($\delta D_{water}$) inside the incubation bottles (+95,195‰) using the following equation:

$$\delta D_{new} = (\varepsilon_{n\text{-alkane-water}} + 1) \times (\delta D_{water} + 1) - 1 \quad (6)$$

From the beginning to the end of the incubation experiment, we have δD values of newly produced *n*-alkanes ($\delta D_{new}$), δD values of existing *n*-alkanes in the control sample ($\delta D_0$), and δD values of the original plus newly produced *n*-alkanes at the end point ($\delta D_{end}$). We can then calculate the relative fractions (f) of newly generated *n*-alkanes and their production rates (r) during this period of time using the following two equations:

$$\delta D_0 \times (1 - f) + \delta D_{new} \times f = \delta D_{end} \quad (7)$$

$$r = f/t \quad (8)$$

where $\delta D_0$ can be obtained from the control sample, and $\delta D_{end}$ be obtained from two incubated samples, $t$ = 1.5 years. The production rates of microbial *n*-alkanes are illustrated in Fig. 3.

The pattern of microbial production rates of different *n*-alkanes corresponds to the degrees of isotopic enrichment. Under aerobic conditions, the production rates of short-chain *n*-alkanes ($C_{18}$ to $C_{21}$) are up to 2.5%/yr, followed by long-chain ($C_{26}$–$C_{31}$) *n*-alkanes, 0.025%/yr for *n*-$C_{26}$, 0.05%/yr for *n*-$C_{27}$ and 0.1%/yr for *n*-$C_{29}$ respectively, and minimal or no new production for mid-chain ($C_{22}$–$C_{25}$) *n*-alkanes (Fig. 3). In contrast, only the short-chain ($C_{18}$ and $C_{19}$) *n*-alkanes display appreciable microbial production under anaerobic conditions, with 0.5%/yr and 0.1%/yr new production. These results display different pattern from the previous research in Zech et al. (2011), where authors claimed that both mid-chain and long-chain *n*-alkanes are produced by microbes in significant quantities. This difference is probably attributed to different microbial communities in the two environmental systems (i.e., peaty soil incubation system in laboratory and foliage litterbag in the field): there could be major differences in synthesis of *n*-alkanes by different microbes (Ladygina et al., 2006).

### 4.3. Implication of microbial production of long-chain n-alkanes in paleoclimate study

In previous studies, long-chain *n*-alkanes (e.g. $C_{29}$, $C_{31}$) in sediments are often thought of as exclusively of leaf-wax origin and widely used to reconstruct paleoclimatic history. Indeed, our incubation results and discussion show that microbial generation of long-chain *n*-alkanes under anaerobic conditions is negligible, suggesting leaf-wax $\delta^{13}C$ and δD are credible paleo-climate or paleo-environment proxies in lacustrine, marine and peatland sediments, as long as leaf wax *n*-alkanes are rapidly buried and experience mostly anaerobic conditions. However, our results also show that the microbial community can produce substantial amount of *n*-$C_{29}$ *n*-alkanes under aerobic conditions, with a generation rate of 0.1%/yr on average. Therefore, the fidelity of using isotopic ratios of long-chain *n*-alkanes as a paleoclimate proxy may strongly depend on the extent of aerobic exposure. For example, leaf wax *n*-alkanes may stay in aerobic soils for a long time before being transported into lacustrine or marine sediment (Douglas et al., 2014). Additionally, the surface of aquatic sediments could stay in relatively aerobic conditions due to the combined effect of low sedimentation rate and extensive activity of benthic community (Supplementary Fig. S2).

Peatlands are usually simplified as two layers: an upper aerobic layer (the acrotelm) and the underlying anaerobic layer (the catotelm). We could evaluate the potential microbial contribution in total $C_{29}$ *n*-alkanes (microbial + leaf wax) under aerobic conditions using the equation below:

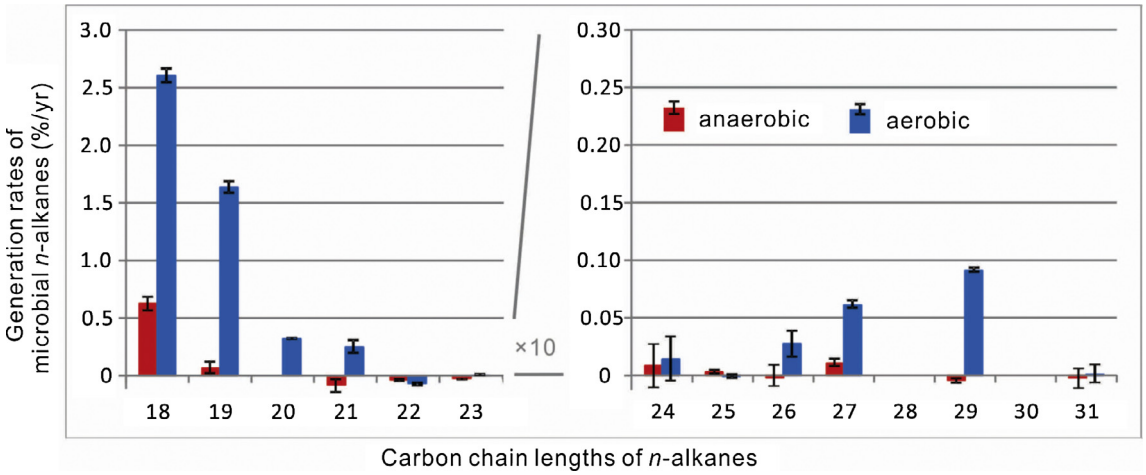


**Fig. 3.** Assessment of microbial production rates for various compounds of *n*-alkanes in aerobic and anaerobic environments respectively.

$$P = \sum_{t=1}^{n}(Mt \times 0.001 \times t)/\left[\sum_{t=1}^{n}(Mt \times 0.001 \times t) + \sum_{t=1}^{n} Mt\right] \quad (9)$$

where $P$ is percentage of microbial *n*-alkanes in total *n*-alkanes, $M_t$ is the mass of terrestrial *n*-alkanes input in the whole year of number $t$, $t$ = 1, 2, 3 ... $n$. When $M_t$ is constant, Eq. (9) becomes Eq. (10):

$$P = (t+1)/(t+2001) \quad (10)$$

The potential microbial contribution to long-chain *n*-alkanes in soil, lake sediments, or peatland, modeled using Eq. (10), is shown in Fig. 4. If leaf wax *n*-alkanes stay in the aerobic environment for a long time, for example 1000 years, the modeled microbial $C_{29}$ *n*-alkane could account for ~1/3 of total $C_{29}$ *n*-alkanes (Fig. 4). The microbial contribution can reach up to 80% if leaf wax *n*-alkanes stay in aerobic conditions for 10,000 years (probably an unlikely scenario in most sedimentary environments). These values may actually represent a minimum estimation since the original leaf wax *n*-alkanes are simultaneously degraded over time when microbes contribute new *n*-alkanes. When degradation of original leaf wax *n*-alkanes is taken into consideration, the percentage of microbial input of long-chain *n*-alkanes to sediments would be even higher.

A surprising finding from our data is that the $C_{31}$ *n*-alkane had a much smaller microbial production rate than the $C_{29}$ *n*-alkane. We do not know if this is universally applicable or it is only specific to our environmental setting and experimental conditions. If this indeed represents a common scenario, the $C_{31}$ *n*-alkane may be a better choice over $C_{29}$ *n*-alkane in sediment for paleoclimate reconstruction. In the sedimentary environments susceptible to prolonged aerobic exposure, we recommend dating the boundary of the aerobic layer to help evaluate the potential aerobic microbial contributions.

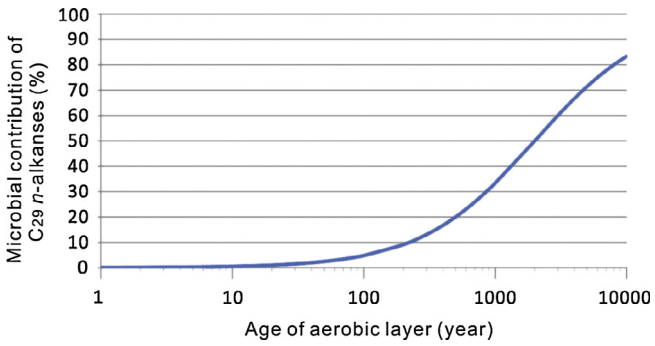


**Fig. 4.** Modeled microbial contribution of $C_{29}$ *n*-alkanes in aerobic layers of soil, lake sediment or peatland environments over timescales of 10–10,000 years.

Our results also show relatively high production of even carbon, $C_{26}$ *n*-alkane under aerobic conditions, indicating microbial *n*-alkanes likely have much smaller odd over even predominance as observed in plants. CPI values of long-chain *n*-alkanes in ancient sediments are often much lower than those from modern plants (Kuhn et al., 2010), which is often interpreted as originating from microbiological or thermal degradation in sediments (Grimalt et al., 1988; Kuhn et al., 2010). However, based on our data, microbial production of even chain length *n*-alkanes under aerobic conditions can also lead to a reduction in CPI values.

## 5. Conclusions

Our incubation experiment demonstrates that distributions and abundances of *n*-alkanes remain virtually unchanged over 1.5 years, consistent with relatively small amounts of microbial *n*-alkane production. Thus, measurements of distributions and abundances for *n*-alkanes do not offer sufficient sensitivity for quantifying the microbial production rates of individual *n*-alkanes.

In contrast, deuterium isotope labeling experiment is an excellent approach to quantify in situ microbial production of *n*-alkanes. The large contrast between the δD values of enrichment water and natural environmental water means even minute amount of microbial production can be assessed with a high degree of accuracy. Under aerobic conditions, the microbial contributions display variable rates for *n*-alkanes with different chain length, which can reach up to 2.5%/yr for short-chain ($C_{18}$–$C_{21}$) *n*-alkanes, and up to 0.1%/yr for long-chain ($C_{27}$–$C_{31}$) *n*-alkanes, and negligible production for mid-chain ($C_{22}$–$C_{25}$) *n*-alkanes. However, under anaerobic conditions, only short-chain ($C_{18}$ and $C_{19}$) *n*-alkanes have a marked microbial contribution, with up to 0.5% per year production rates.

The absence of microbial generation of long-chain *n*-alkanes in anaerobic condition adds credibility to leaf-wax $\delta^{13}C$ and δD as paleo-climate or paleo-environment proxies in lacustrine, marine and peatland sediments, as long as leaf wax derived *n*-alkanes are rapidly buried and experience mostly anaerobic conditions. However, in cases where prolonged aerobic exposure occurs (e.g., leaf waxes having long residence time in aerobic soils), substantial microbial contribution to long-chain *n*-alkanes can occur, with a rate up to 30% over 1000 years. Our preliminary results also show $C_{29}$ *n*-alkane may be produced in greater quantity than $C_{30}$ *n*-alkane by aerobic microbes.

## Acknowledgments

This work was supported by a National Science Foundation of United States award to Y.H. (EAR-1122749, PLR-1503846, EAR-1502455), grants from the National Natural Science Foundation of China (Grant No. 41702364 award to G.L., Grant No. Y511191046 award to Y.H., Grant No. 41572328 award to H.D., Grant No. 41376046 award to L.L.), "the Fundamental Research Funds for the Central Universities" award to G.L. (Grant No. 2652017044), and financial support from a program of China Scholarship Council award to G.L. (CSC No. 201406400012). We are grateful to two anonymous reviewers whose comments significantly improved the quality of the manuscript.

## Appendix A. Supplementary material

Supplementary data associated with this article can be found, in the online version, at https://doi.org/10.1016/j.orggeochem.2017.10.005.

*Associate Editor*—**Stefan Schouten**

## References

Bush, R.T., McInerney, F.A., 2013. Leaf wax *n*-alkane distributions in and across modern plants: implications for paleoecology and chemotaxonomy. Geochimica et Cosmochimica Acta 117, 161–179.
Castañeda, I.S., Schouten, S., 2011. A review of molecular organic proxies for examining modern and ancient lacustrine environments. Quaternary Science Reviews 30, 2851–2891.
Douglas, P.M.J., Pagani, M., Eglinton, T.I., Brenner, M., Hodell, D.A., Curtis, J.H., Ma, K. F., Breckenridge, A., 2014. Pre-aged plant waxes in tropical lake sediments and their influence on the chronology of molecular paleoclimate proxy records. Geochimica et Cosmochimica Acta 141, 346–364.
Eglinton, G., Hamilton, R.J., 1967. Leaf epicuticular waxes. Science 156, 1322–1335.
Eglinton, T.I., Eglinton, G., 2008. Molecular proxies for paleoclimatology. Earth and Planetary Science Letters 275, 1–16.
Fuller, M., Huang, Y., 2003. Quantifying hydrogen-deuterium exchange of meteoritic dicarboxylic acids during aqueous extraction. Meteoritics & Planetary Science 38, 357–363.
Gao, L., Burnier, A., Huang, Y., 2012. Quantifying instantaneous regeneration rates of plant leaf waxes using stable hydrogen isotope labeling. Rapid Communications in Mass Spectrometry 26, 115–122.
Gao, L., Hou, J., Toney, J., MacDonald, D., Huang, Y., 2011. Mathematical modeling of the aquatic macrophyte inputs of mid-chain *n*-alkyl lipids to lake sediments: implications for interpreting compound specific hydrogen isotopic records. Geochimica et Cosmochimica Acta 75, 3781–3791.
Grimalt, J.O., Torras, E., Albaigés, J., 1988. Bacterial reworking of sedimentary lipids during sample storage. Organic Geochemistry 13, 741–746.
Hou, J., D'Andrea, W.J., Huang, Y., 2008. Can sedimentary leaf waxes record D/H ratios of continental precipitation? Field, model, and experimental assessments. Geochimica et Cosmochimica Acta 72, 3503–3517.
Huang, Y., Clemens, S.C., Liu, W., Wang, Y., Prell, W.L., 2007. Large-scale hydrological change drove the late Miocene $C_4$ plant expansion in the Himalayan foreland and Arabian Peninsula. Geology 35, 531–534.
Huang, Y., Shuman, B., Wang, Y., Webb, T., 2002. Hydrogen isotope ratios of palmitic acid in lacustrine sediments record late Quaternary climate variations. Geology 30, 1103–1106.
Huang, Y., Shuman, B., Wang, Y., Webb, T., 2004. Hydrogen isotope ratios of individual lipids in lake sediments as novel tracers of climatic and environmental change: a surface sediment test. Journal of Paleolimnology 31, 363–375.
Huang, Y., Street-Perrott, F.A., Metcalfe, S.E., Brenner, M., Moreland, M., Freeman, K. H., 2001. Climate change as the dominant control on glacial-interglacial variations in $C_3$ and $C_4$ plant abundance. Science 293, 1647–1651.
Huang, Y., Street-Perrott, F.A., Perrott, R.A., Metzger, P., Eglinton, G., 1999. Glacial-interglacial environmental changes inferred from molecular and compound-specific $\delta^{13}C$ analyses of sediments from Sacred Lake, Mt. Kenya. Geochimica et Cosmochimica Acta 63, 1383–1404.
Jones, J.G., 1969. Studies on lipids of soil micro-organisms with particular reference to hydrocarbons. Microbiology 59, 145–152.
Konecky, B., Russell, J., Huang, Y., Vuille, M., Cohen, L., Street-Perrott, F.A., 2014. Impact of monsoons, temperature, and $CO_2$ on the rainfall and ecosystems of Mt. Kenya during the Common Era. Palaeogeography, Palaeoclimatology, Palaeoecology 396, 17–25.
Konecky, B.L., Russell, J.M., Johnson, T.C., Brown, E.T., Berke, M.A., Werne, J.P., Huang, Y., 2011. Atmospheric circulation patterns during late Pleistocene climate changes at Lake Malawi, Africa. Earth and Planetary Science Letters 312, 318–326.
Kuhn, T.K., Krull, E.S., Bowater, A., Grice, K., Gleixner, G., 2010. The occurrence of short-chain *n*-alkanes with an even over odd predominance in higher plants and soils. Organic Geochemistry 41, 88–95.
Ladygina, N., Dedyukhina, E.G., Vainshtein, M.B., 2006. A review on microbial synthesis of hydrocarbons. Process Biochemistry 41, 1001–1014.
Lichtfouse, E., Berthier, G., Houot, S., Barriuso, E., Bergheaud, V., Vallaeys, T., 1995. Stable carbon isotope evidence for the microbial origin of $C_{14}$–$C_{18}$ *n*-alkanoic acids in soils. Organic Geochemistry 23, 849–852.
Meyers, P.A., 2003. Applications of organic geochemistry to paleolimnological reconstructions: a summary of examples from the Laurentian Great Lakes. Organic Geochemistry 34, 261–289.
Orò, J., Laseter, J.L., Weber, D., 1966. Alkanes in fungal spores. Science 154, 399–400.
Osburn, M.R., Sessions, A.L., Pepe-Ranney, C., Spear, J.R., 2011. Hydrogen-isotopic variability in fatty acids from Yellowstone National Park hot spring microbial communities. Geochimica et Cosmochimica Acta 75, 4830–4845.
Pagani, M., Pedentchouk, N., Huber, M., Sluijs, A., Schouten, S., Brinkhuis, H., Sinninghe Damsté, J.S., Dickens, G.R., Jakobsson, M.Expedition 302 Scientists, 2006. Arctic hydrology during global warming at the Palaeocene/Eocene thermal maximum. Nature 442, 671–675.
Pancost, R.D., Baas, M., van Geel, B., Sinninghe Damsté, J.S., 2002. Biomarkers as proxies for plant inputs to peats: an example from a sub-boreal ombrotrophic bog. Organic Geochemistry 33, 675–690.
Polissar, P.J., Freeman, K.H., Rowley, D.B., McInerney, F.A., Currie, B.S., 2009. Paleoaltimetry of the Tibetan Plateau from D/H ratios of lipid biomarkers. Earth and Planetary Science Letters 287, 64–76.
Rach, O., Brauer, A., Wilkes, H., Sachse, D., 2014. Delayed hydrological response to Greenland cooling at the onset of the Younger Dryas in western Europe. Nature Geoscience 7, 109–112.
Reeves, E.P., Seewald, J.S., Sylva, S.P., 2012. Hydrogen isotope exchange between *n*-alkanes and water under hydrothermal conditions. Geochimica et Cosmochimica Acta 77, 582–599.
Russell, J.M., Vogel, H., Konecky, B.L., Bijaksana, S., Huang, Y.S., Melles, M., Wattrus, N., Costa, K., King, J.W., 2014. Glacial forcing of central Indonesian hydroclimate since 60,000 y BP. Proceedings of the National Academy of Sciences of the United States of America 111, 5100–5105.
Sachse, D., Billault, I., Bowen, G.J., Chikaraishi, Y., Dawson, T.E., Feakins, S.J., Freeman, K.H., Magill, C.R., McInerney, F.A., van der Meer, M.T.J., Polissar, P., Robins, R.J., Sachs, J.P., Schmidt, H.L., Sessions, A.L., White, J.W.C., West, J.B., Kahmen, A., 2012. Molecular paleohydrology: interpreting the hydrogen-isotopic composition of lipid biomarkers from photosynthesizing organisms. Annual Review of Earth and Planetary Sciences 40, 221–249.
Schefuß, E., Kuhlmann, H., Mollenhauer, G., Prange, M., Pätzold, J., 2011. Forcing of wet phases in southeast Africa over the past 17,000 years. Nature 480, 509–512.
Schefuß, E., Schouten, S., Schneider, R.R., 2005. Climatic controls on central African hydrology during the past 20,000 years. Nature 437, 1003–1006.
Schimmelmann, A., Lewan, M.D., Wintsch, R.P., 1999. D/H isotope ratios of kerogen, bitumen, oil, and water in hydrous pyrolysis of source rocks containing kerogen types I, II, IIS, and III. Geochimica et Cosmochimica Acta 63, 3751–3766.
Sessions, A.L., Jahnke, L.L., Schimmelmann, A., Hayes, J.M., 2002. Hydrogen isotope fractionation in lipids of the methane-oxidizing bacterium *Methylococcus capsulatus*. Geochimica et Cosmochimica Acta 66, 3955–3969.
Sessions, A.L., Sylva, S.P., Summons, R.E., Hayes, J.M., 2003. Isotopic exchange of carbon-bound hydrogen over geologic timescales. Geochimica et Cosmochimica Acta 68, 1545–1559.
Thomas, E.K., Briner, J.P., Ryan-Henry, J.J., Huang, Y., 2016. A major increase in winter snowfall during the middle Holocene on western Greenland caused by reduced sea ice in Baffin Bay and the Labrador Sea. Geophysical Research Letters 43, 5302–5308.
Tierney, J.E., Russell, J.M., Huang, Y.S., Sinninghe Damsté, J.S., Hopmans, E.C., Cohen, A.S., 2008. Northern hemisphere controls on tropical southeast African climate during the past 60,000 years. Science 322, 252–255.
Tipple, B.J., Pagani, M., 2010. A 35 Myr North American leaf-wax compound-specific carbon and hydrogen isotope record: implications for $C_4$ grasslands and hydrologic cycle dynamics. Earth and Planetary Science Letters 299, 250–262.
Tipple, B.J., Pagani, M., Krishnan, S., Dirghangi, S.S., Galeotti, S., Agnini, C., Giusberti, L., Rio, D., 2011. Coupled high-resolution marine and terrestrial records of carbon and hydrologic cycles variations during the Paleocene-Eocene Thermal Maximum (PETM). Earth and Planetary Science Letters 311, 82–92.
Tu, T.T.N., Egasse, C., Zeller, B., Bardoux, G., Biron, P., Ponge, J., David, B., Derenne, S., 2011. Early degradation of plant alkanes in soils: a litterbag experiment using $^{13}C$-labelled leaves. Soil Biology & Biochemistry 43, 2222–2228.
Wang, X., Huang, X., Sachse, D., Ding, W., Xue, J., 2016. Molecular paleoclimate reconstructions over the last 9 ka from a peat sequence in South China. PLoS One 11, e0160934.
Wang, Y., Sessions, A.L., 2008. Memory effects in compound-specific D/H analysis by gas chromatography/pyrolysis/isotope-ratio mass spectrometry. Analytical Chemistry 80, 9162–9170.
Wedeking, K., Hayes, J., 1983. Exchange of oxygen isotopes between water and organic material. Chemical Geology 41, 357–370.
Weete, J.D., 1972. Aliphatic hydrocarbons of the fungi. Phytochemistry 11, 1201–1205.
Zech, M., Pedentchouk, N., Buggle, B., Leiber, K., Kalbitz, K., Markovic, S.B., Glaser, B., 2011. Effect of leaf litter degradation and seasonality on D/H isotope ratios of *n*-alkane biomarkers. Geochimica et Cosmochimica Acta 75, 4917–4928.

Zech, M., Krause, T., Sascha, M., Faust, D., 2013. Incorrect when uncorrected: reconstructing vegetation history using *n*-alkane biomarkers in loess-paleosol sequences – a case study from the Saxonian loess region, Germany. Quaternary International 296, 108–116.

Zhang, X., Gillespie, A.L., Sessions, A.L., 2009. Large D/H variations in bacterial lipids reflect central metabolic pathways. Proceedings of the National Academy of Sciences of the United States of America 106, 12580–12586.